Desalination and Water Treatment
www.deswater.com

doi: 10.5004/dwt.2018.22321

114 (2018) 192–204
May

Studies on the remediation of chromium(VI) from simulated wastewater using novel biomass of *Pinus kesiya* cone

Ajmani Abhishek[a], Narayanan Saranya[b], Patra Chandi[a], Narayanasamy Selvaraju[a,*]

[a]*Department of Biosciences and Bioengineering, Indian Institute of Technology Guwahati, Guwahati, Assam, India, Tel. +91-361-2583210; Fax: +91-361-2582249; emails: selva@iitg.ernet.in (N. Selvaraju), a.ajmani@iitg.ernet.in (A. Ajmani), chandipatra.lpu@gmail.com (P. Chandi)*
[b]*Department of Chemical Engineering, National Institute of Technology Calicut, Kozhikode, Kerala, India, email: swaranya2218@gmail.com*

Received 18 January 2018; Accepted 5 April 2018

ABSTRACT

Hexavalent chromium pollution in water puts forward a huge threat to environment and human health. Conventional methods of heavy metal removal from water generate toxic by-products, which mandate the use of efficient and alternative biosorbent-based strategies. In this study, a novel biosorbent *Pinus kesiya* cone biomass has been investigated for the hexavalent chromium removal from aqueous solutions. The biosorbent characteristics have been analyzed using Brunauer–Emmett–Teller, Fourier transform infrared spectrometry, field emission scanning electron microscopy–energy dispersive X-ray spectrometry, thermogravimetric analysis, X-ray diffraction and electron spin resonance analyses. Parameters influencing the biosorption process were optimized as pH 2.0, temperature 303 K, initial Cr(VI) concentration 500 mg/L, biosorbent dose 0.5 g/L, biosorbent size of <300 μm and contact time 210 min. Langmuir isotherm fitted experimental data better than the Freundlich and Dubinin–Radushkevitch isotherm showed that the biosorption followed monolayer adsorption. Maximum biosorption capacity calculated by Langmuir adsorption isotherm was found to be 73.96 mg/g. Pseudo-second-order kinetics was found to have a better fit than the other kinetic models analyzed. Thermodynamic studies revealed that the biosorption process occurs in spontaneous, stable and exothermic manner. Desorption and regeneration studies showed that the biosorbent is reusable and an ecofriendly option for Cr(VI) removal from aqueous solutions. Breakthrough experiment on Cr(VI) biosorption by *P. kesiya* cone biomass was carried out in continuous packed bed column. These interesting findings on Cr(VI) biosorption by *P. kesiya* cone biomass vouches for its potential application as an alternative biosorbent for Cr(VI) removal.

Keywords: Pinus kesiya cone biomass; Isotherm; Kinetics; Desorption; Chromium; ESR; Langmuir; Freundlich; Pseudo-first order; Pseudo-second order

1. Introduction

Clean water is an essential need of all living organisms. However, the water available in the nature in the form of rivers and other flowing sources has been highly polluted owing to the disposal of wastewater generated from the industry. The polluted water directly or indirectly carries great risk to the health of all organisms related to the water source. Of the several pollutants present in the wastewater, heavy metals constitute one of the major pollutants being discharged into the rivers and other sources [1,2]. Chromium is a heavy metal, exists in trivalent form Cr(III) and hexavalent form Cr(VI). Although chromium in trivalent oxidation state is not so hazardous, chromium in hexavalent oxidation state is highly toxic, causes pulmonary congestion, skin irritation, ulcers, nerve damage and cancer when present at a level more than 0.05 mg/L in drinking water due to higher permeability in cells and reactivity [3,4]. Chromium exists in hexavalent form as stable dichromate ($Cr_2O_7^{2-}$) and chromate ($HCrO^{4-}$) ions in aqueous solutions [5]. The primary sources of chromium in wastewater are attributed to industrial activities such as leather tanning, electroplating, wood preservation, photolithographic industries, refineries and chemical

* Corresponding author.

production industries [6]. The high severity of chromium on living world makes it inevitable to reduce the levels of chromium in water.

Conventional effluent treatment methods such as sedimentation, coagulation, membrane separation, evaporation, extraction and precipitation are not efficient in sequestration of heavy metals from water as compared with biosorption and photocatalysis owing to certain disadvantages such as sludge production, high cost, non-reusability and difficulty in metal recovery [7–11]. Adsorption, being a simple and cost-effective procedure, has been investigated from the past several decades for sequestration of various pollutants including heavy metals [12–16]. Various types of adsorbents such as dead microorganisms like *Rhizopus arrhizus* [17], *Oedogonium hatei* [18], *Rhizoclonium hookeri* [19] and *Sargassum polycystum* [20], lignocellulosic materials like walnut hull [21] and *Ficus carica* bast fibers [22] and synthetic chemical compounds like chitosan-crosslinked-poly(alginic acid) nanohydrogel [23] have been explored for removing chromium in the recent years due to their affordability, availability, reusability and degradability in comparison with commercially used adsorbents.

Pinus kesiya which belongs to the family Pinaceae, is one of the most widely distributed pines in Asia [24]. In India, *P. kesiya* trees occur mainly in North East region except the states of Assam and Tripura [25]. The cone structures of the pine are hard in nature and the scales of these cones are rich in cellulose, lignin, hemicellulose and tannin [24]. The cone structures of pine are easily available in abundant amount and cost negligible. Lignocellulosic materials have been found to have high Cr(VI) removal capacity. To our knowledge, as per the literature survey, there is no reported industrial use of *P. kesiya* cones. However, the local people of North East India use the female cones of *P. kesiya* as fuel [25].

Consequently, the aim of this study was to utilize *P. kesiya* cone biomass (PKB) for the adsorption of Cr(VI) from aqueous synthetic waste solutions. Parameters having influence over the biosorption process were optimized for maximum Cr(VI) removal. Isotherm, kinetics and thermodynamic parameters were determined to study the adsorption behavior of Cr(VI) on PKB surface. Theoretical studies were done by fitting data for various isotherm models such as Langmuir and Freundlich adsorption isotherm and kinetic models such as pseudo-first-order and pseudo-second-order kinetic models. Desorption and regeneration studies were carried out to check the reusability of the biomass. Continuous column study was subsequently performed to estimate the utilization efficiency of PKB for removing Cr(VI) from aqueous solutions.

2. Materials and methods

2.1. Preparation of stock solution

Potassium dichromate (2.828 g) was dissolved in 1,000 mL deionized water to prepare 1,000 ppm stock solution. Working standards of 100–500 mg/L solutions were made by appropriate dilutions in deionized water.

2.2. Preparation of biosorbent

PKB was collected from Nehru Park, Shillong, Meghalaya, India. The collected cones were washed thrice with deionized water before keeping in hot air oven at 353 K for drying. Pine cones were ground in a mixer-grinder before separating them into three different particle size range (<300, 300–425 and 425–600 μm). Sieved pine cone biomass was kept in sealed bags for further use.

2.3. Characterization of biosorbent

Point of zero charge (PZC) analysis of PKB was carried out by agitating 0.5 g of biosorbent in 0.1 M KNO_3 of different pH (pH 2.0–9.0) for 24 h at 313 K. pH of the solutions was adjusted using 0.1 N HCl and 0.1 N NaOH measured by a digital pH meter (PB-11, Sartorius, Germany). The variation in the pH between initial and final state was measured and plotted versus the initial pH. The point of intersection at which DpH is zero was considered as PZC.

Surface characteristics of the biosorbent were determined using field emission scanning electron microscopy (FESEM; Zeiss, Sigma, Germany). Energy dispersive X-ray spectrometry (EDX; Zeiss, Sigma, Germany) was done for PKB before and after Cr(VI) adsorption. Functional groups involved in the Cr(VI) adsorption were identified using Fourier transform infrared spectrometry (FTIR; Spectrum Two, PerkinElmer, USA). Surface area and pore size of PKB were measured by surface area and pore size analyzer (Autosorb-IQ MP, Quantachrome, USA). Thermal stability of the biosorbent was analyzed by subjecting the biosorbent to temperatures in the range of 25°C–800°C by increasing temperature at a rate of 10°C min^{-1} in N_2 atmosphere using high temperature DSC/TG system (TG; STA449F3A00, Netzsch, Bavaria, Germany).

The X-ray diffraction (XRD) studies were performed by using high-power TTRAX diffractometer (TTRAX, Rigaku, Japan) analytical instrument run at 50 kV and a current of 100 mA with Cu radiation (λ = 1.5406). A continuous scan mode was opted to collect 2θ data from 10° to 70° at a scan speed of 4 min^{-1}.

Electron spin resonance (ESR) analysis was conducted at room temperature in powder form using JEOL Spectrometer (JESFA200, JEOL, Japan) operating at X-band frequency (ν = 9.4 GHz) with 100 kHz magnetic field modulation.

Biosorption parameter optimization experiments were performed in 250 mL screw capped conical flasks with 50 mL working volume. Agitation of the PKB and Cr(VI) solution was carried out using incubator shaker (Orbitek, Scigenics Biotech, India) at 303 K. Various parameters such as biosorbent dose (0.5–5 g/L), biosorbent size (<300–600 μm), pH (2.0–5.0), temperature (303–323 K) and initial chromium concentration (100–500 mg/L) were optimized for maximum Cr(VI) removal. Residual Cr(VI) concentration in the filtrate from samples after contacting with the biosorbent was measured using a UV-Visible spectrophotometer (GeneQuant 1300, GE, USA) after addition of 1,5-diphenyl carbazide in acidic conditions at 540 nm. The percentage removal of Cr(VI) was calculated by using the equation:

$$\% \text{ Removal} = \left(\frac{C_o - C_t}{C_o} \right) \times 100 \quad (1)$$

where C_o is the initial Cr(VI) concentration (mg/L), C_e is the equilibrium Cr(VI) concentration at time 't' (mg/L).

The adsorption capacity q_t of PKB was calculated using the equation:

$$q_t = \frac{\left(C_o - C_t\right) \times \mathrm{V}}{m} \tag{2}$$

where C_t is the Cr(VI) concentration at time 't' (mg/L), 'm' is the mass of PKB (g) and 'V' is the volume of Cr(VI) solution (mL).

2.4. Desorption and regeneration studies

Desorption studies were carried out using 0.1 N NaOH as desorbing agent. The biosorbent after adsorption of Cr(VI) was filtered using Whatmann filter paper No. 1 and added in 50 mL of 0.1 N NaOH solution and measured for Cr(VI) at regular intervals till maximum desorption occurred. The regenerated biosorbent was subjected to Cr(VI) adsorption studies to check the efficacy of used PKB. Desorption percentages were calculated using the following equation:

$$\%\ \text{Desorption} = \frac{C_{\text{des}}}{C_{\text{ads}}} \times 100 \tag{3}$$

where C_{des} is the concentration of chromium desorbed at time 't' (mg/L), C_{ads} is the concentration of chromium adsorbed at the same time 't' (mg/L).

2.5. Column studies

Continuous mode of Cr(VI) biosorption was performed with PKB packed as bed in glass column with dimensions of internal diameter 1 cm and length 15 cm. The packed column was washed several times with deionized water, loaded with glass wool at the bottom of the column approximately to a height of 1 cm. Glass beads of 3 mm diameter were loaded next to the glass wool to a height of 1.5 cm. Approximately, 4.5 g of PKB was packed to 10 cm height in the column. Cr(VI) solution (100 mg/L) was passed through the packed bed column by a peristaltic pump (PP-20-EX, Miclins, India) at the flow rate of 5 mL/min. Up flow movement of Cr(VI) solution was chosen in order to attain even distribution throughout the packed bed of PKB. Sample of 20 mL from the outlet was collected at fixed time duration, filtered and estimated for Cr(VI) until equilibrium attained. Effective volume of Cr(VI) solution that can be treated using PKB was determined by plotting a breakthrough curve between C_t/C_o and volume treated.

3. Results and discussion

3.1. Biosorbent characterization

PZC of the biosorbent was calculated to be pH 4.0 (Fig. 1), which showed that the biosorbent surface is prone to anionic Cr(VI) binding below this critical pH. Brunauer–Emmett–Teller (BET) analysis presented in Table 1 showed that the biosorbent has considerable surface area with pores in it which is suitable for metal binding.

The TG curve (Fig. 2) showed that two weight loss stages occurred in the process: when the temperature is below 150°C,

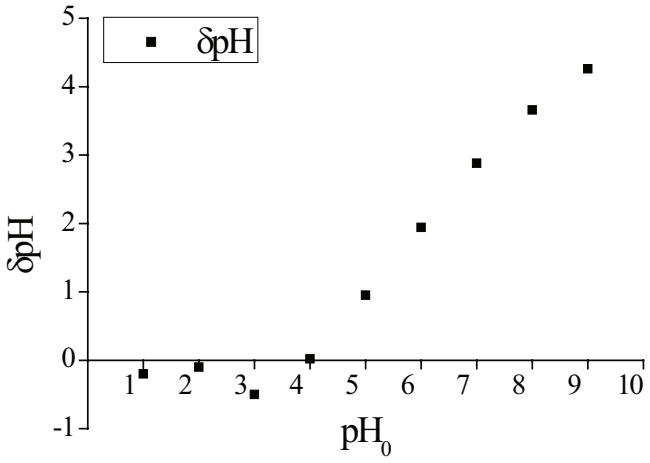

Fig. 1. Determination of PZC (PKB dose 0.5 g in 40 mL of 0.1 N KNO_3 agitated for 24 h).

Table 1
BET analysis of PKB

Parameters	Values
Total pore volume (cc/g)	1.084×10^{-2}
Surface area (m^2/g)	3.938
Pore diameter (nm)	3.312
Average pore diameter (nm)	1.10092

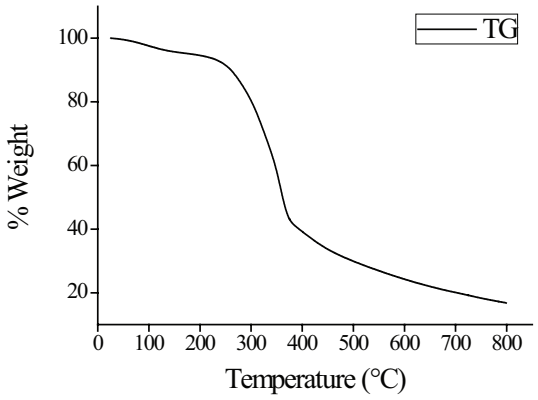

Fig. 2. Determination of stability of the raw biosorbent (PKB) using TG in the temperature range of 25°C–800°C.

the reduction in weight is primarily due to moisture loss. From 240°C to 375°C, the weight loss was owing to pyrolysis of PKC. From 375°C to 465°C, there was a relatively less sharp decrease; however, a weight loss of 10% occurred in this span of temperature change. From this temperature profile, the carbonation temperature may be chosen as 465°C to produce stable activated carbon for further studies. In a previous report, Li et al. also reported that TG curve for pine cone showed two weight loss stages: from 200°C to 400°C, the weight loss was mainly due to the pyrolysis of pine cone shells; from 400°C to 500°C, the loss rate of weight became slow [26].

FESEM micrographs of PKB before Cr(VI) treatment (Fig. 3(a)) show that the surface of the biosorbent is rough, striated with ridges and pores upon them. Similar observation has been noticed in several plant-based biosorbents such as *Caryota urens* [27], *Annona reticulata* Linn. [28] and *Colocasia esculenta* [29] exhibiting surface properties conducive for hexavalent chromium removal. FESEM micrograph of the PKB after Cr(VI) adsorption is shown in Fig. 3(b). The surface of the biosorbent was observed to contain smaller particles adhering and occupying the pores.

EDX analysis (Figs. 3(c) and (d)) revealed that these particulates were indeed the adsorbed Cr(VI) attesting its applicability as a suitable biosorbent. There were no peaks found (Fig. 3(c)) for chromium ions from any spectral lines of X-ray energies before adsorption. However, after Cr(VI) adsorption, there are distinct peaks for chromium at energy levels 0.57, 5.4 and 5.9 keV which clearly reveals that chromium has been adsorbed over the surface of the PKB.

Surface functional groups of the biosorbent have been found to play a role in adsorption of Cr(VI) by analyzing the FTIR spectrum before and after adsorption. The shift in the wavenumber from 3,396.53 to 3,385.53 cm^{-1} indicated the association of surface –OH group in Cr(VI) adsorption on PKB (Fig. 4). The wavenumber shift from 2,925.14 to 2,916.62 cm^{-1} indicated the involvement of C–H (stretching). Wavenumber shift from 1,632.96 to 1,620.84 cm^{-1} represented the C=C (stretching). Involvement of alkenes is often represented by several researchers in the use of plant-based lignocellulosic wastes for removal of heavy metals [30]. The minor shift in wavenumber at 1,057.65, 1,268.24 and 1,730.33 cm^{-1} indicates the non-involvement of C–O (stretching), CN (stretching) and C=O in Cr(VI) adsorption. From the FTIR analysis done, the functional moieties interacting in the biosorption of chromium onto the surface of the PKB were determined as hydroxyl, alkenes and alkyl groups.

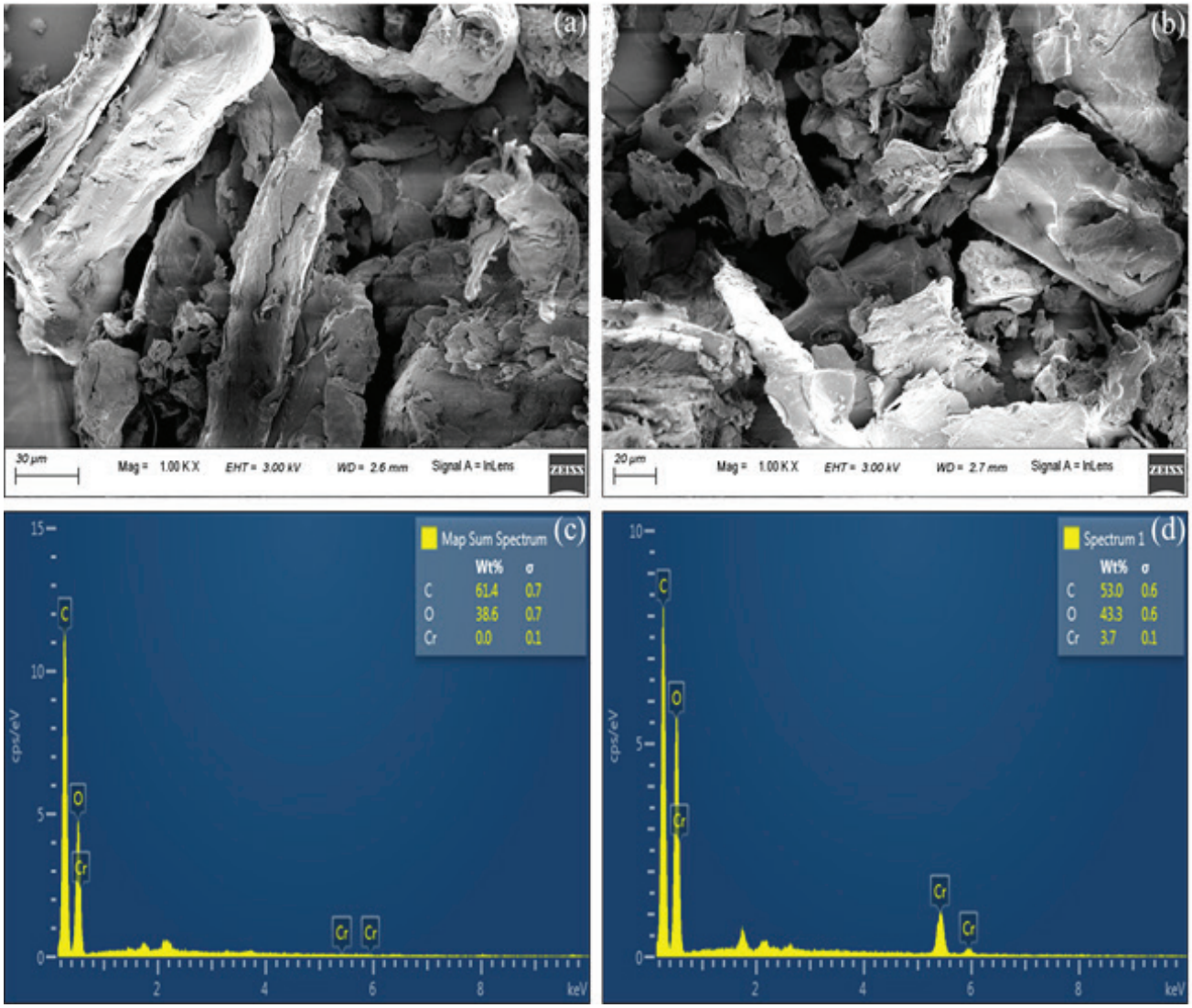

Fig. 3. SEM image of (a) pine cone particles size <300 µm (×1,000) and (b) chromium-loaded pine cone particles size <300 µm (×1,000). EDX image of (c) pine cone particles size <300 µm (×1,000) and (d) chromium-loaded pine cone particles size <300 µm (×1,000).

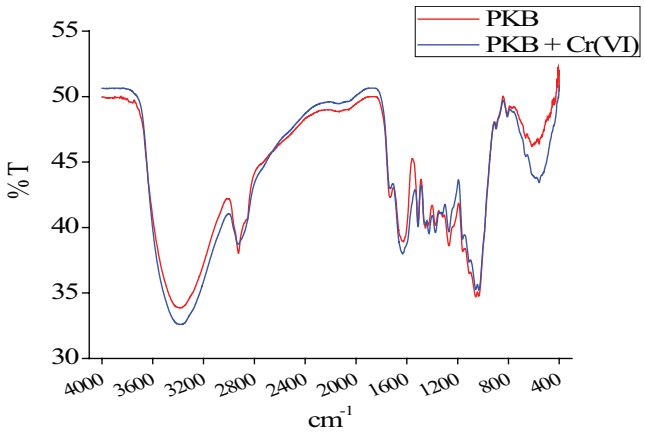

Fig. 4. FTIR spectral analysis of PKB before and after Cr(VI) adsorption.

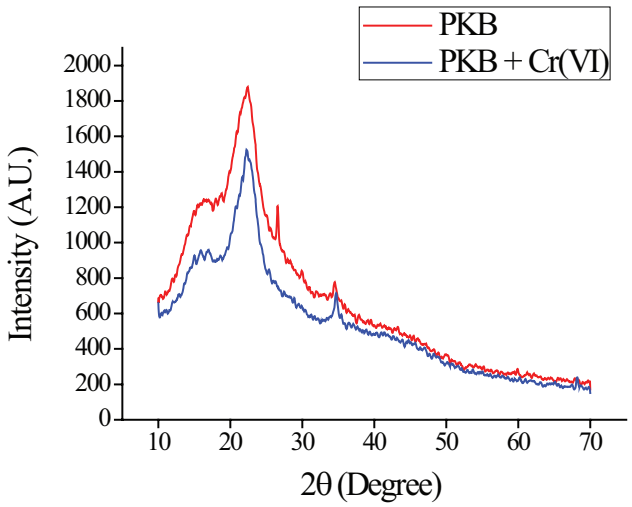

Fig. 5. XRD analysis of PKB before and after Cr(VI) adsorption.

XRD was carried out to determine the crystallinity of PKB and oxidation state of chromium (Fig. 5). The peaks in the spectra are broad; hence, it shows the amorphous nature of the PKB. Characteristic peaks of trivalent oxidation state of chromium were not found. From the XRD spectrum, it was observed that there was no change in oxidation state of chromium from hexavalent to trivalent upon adsorption of chromium onto PKB. However, the degree of reduction of Cr(VI) to Cr(III) may be less [31]. The mechanism of the biosorption of chromium may involve electrostatic interactions.

To further investigate the mechanism of adsorption, ESR was performed (Fig. 6). The gValue of trivalent chromium ($Cr(NO_3)_3.9H_2O$) was found to be 1.98. The gValue of PKB after chromium adsorption was found to be 1.99. The ESR spectra shows that there is very less or negligible amount of Cr(VI) reduced to Cr(III) [32].

3.2. Influence of biosorbent size

The influence of biosorbent size on Cr(VI) removal was studied using three different size ranges <300, 300–450, 456–600 μm at pH 2.0, temperature 303 K, biosorbent dose of 0.25 g in 50 mL of 100 mg/L chromium solution. Fig. 7(a) clearly shows that smaller sized particles of <300 μm presented higher Cr(VI) removal percentage of 99.10 than that of other larger sized particles utilized. This may be attributed to the larger surface area contribution by the smaller sized particles with the exposure of more number of functional groups prone to Cr(VI) binding [32]. The chromium removal percentage gradually declined with the increase in the particle size owing to the decreased surface area and surface characteristics.

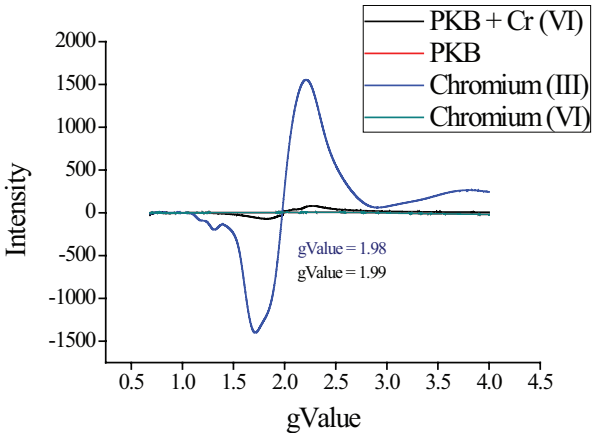

Fig. 6. Electron spin resonance spectra of PKB.

3.3. Influence of biosorbent dose

Influence of PKB dose was analyzed by using 0.5–5.0 g of biosorbent of size less than 300 μm with 50 mL solution of 100 mg/L initial chromium concentration maintained at pH 2.0, temperature 303 K and agitation speed 100 rpm. Fig. 7(b) shows that the chromium removal percentage sharply increased with increase in the dose of PKB from 0.5 to 3.0 g. This may be due to more surface area and reactive functional groups available with the increase in the biosorbent [33]. However, increase in chromium removal percentage was less with 3.5 g of PKB. Further, there was no considerable change in chromium removal percentage on increasing the PKB dose from 3.5 to 5.0 g. The maximum chromium removal was 99.33% with 5.0 g of PKB. On increasing the PKB dose beyond 3.5 g, due to the less availability of surface area per unit weight of PKB, there was relatively less increase in the removal percentage which resulted in equilibrium.

3.4. Effect of pH

Influence of pH upon Cr(VI) adsorption was examined in the pH range of 2.0–7.0 at 303 K with 100 mg/L of Cr(VI) solution, optimum dose and size of biosorbent. It was found that at lower pH 2.0, maximum chromium adsorption occurred with magnitude of 53.88 mg/g. As the pH increased to 3.0, 4.0 and 5.0, the adsorption capacity got decreased to 35.6, 27.4 and 16.6 mg/g, respectively, as shown in Fig. 7(c). With further increase in pH, the adsorption capacity got further decreased. The obvious fact behind this is that hydrogen chromate

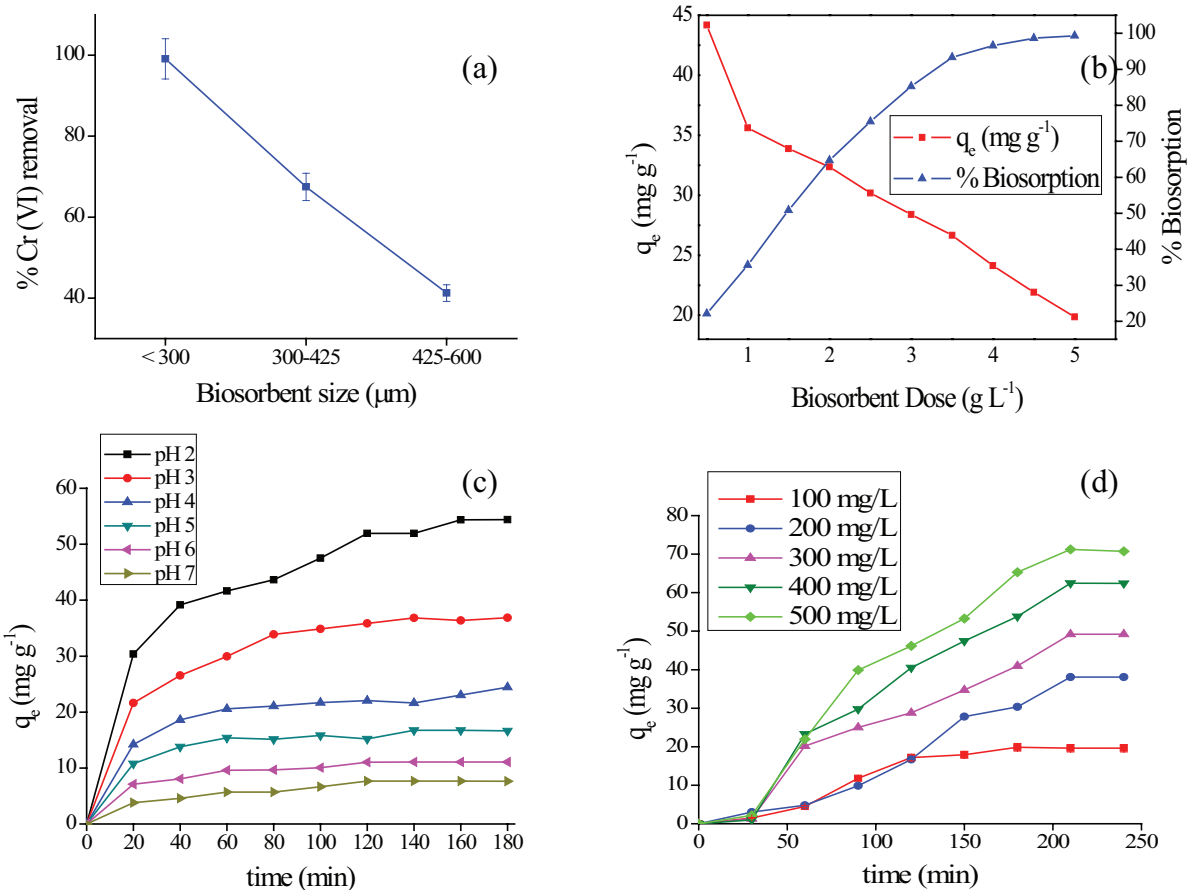

Fig. 7. (a) Influence of biosorbent size on Cr(VI) removal. (b) Plot showing influence of biosorbent dose upon removal percentage and adsorption capacity (C_o 100 mg/L, contact time 3 h, agitation speed 100 rpm, pH 2.0, temperature 303 K). (c) Influence of pH on Cr(VI) adsorption using PKB. (d) Influence of contact time and Cr(VI) concentration.

($HCrO_4^-$), chromate (CrO_4^{2-}) and dichromate ($Cr_2O_7^{2-}$) ions being anionic tend to attract positively charged ions in solution. At lower pH solutions, the biosorbent surface becomes more protonated and hence there is an electrostatic interaction between chromium ions and positively charged ions of the biosorbent resulted in increased adsorption capacity. The surface of the biosorbent becomes less protonated with the increase in pH and repels off the anionic chromium ions [34].

3.5. Influence of contact time and initial Cr(VI) concentration

The time at which equilibrium adsorption capacity attained was analyzed for different Cr(VI) concentrations (100–500 mg/L) at optimized sorbent size, dose, pH 2.0 at 100 rpm and 303 K. The maximum adsorption capacity of 71.24 mg/g of the biosorbent was attained for 500 mg/L Cr(VI) solution at 210 min. The equilibrium adsorption capacity gradually decreased with decrease in Cr(VI) concentration and attained minimum of 19.60 mg/g for 100 mg/L Cr(VI) solution. This may be due to the increased driving force between Cr(VI) and functional groups of biosorbent owing to the development of concentration gradient [35]. The optimum time for biosorbent to attain equilibrium was 210 min, after which there was no considerable increase in adsorption capacity for all the Cr(VI) concentrations (Fig. 7(d)). This might be due to the exhaustion of active sites for the adsorption of Cr(VI) ions to attach with the biosorbent surface [36].

3.6. Isotherm studies

Isotherm studies informed about the nature of interaction amid the biosorbent and Cr(VI) ions. Isotherm studies were done using various two parameter isotherm models such as Langmuir, Freundlich and Dubinin–Radushkevitch (DR) models with the experimental equilibrium adsorption capacity data at different initial concentration of Cr(VI) solution.

3.6.1. Langmuir isotherm model

Langmuir isotherm model assumes monolayer attachment of ions over the surface of the biosorbent with no interaction between the adjacent ions. Further, the model assumes that all the ions covering the monolayer of the biosorbent surface have same affinity [37,38]. The linear form of the Langmuir model is written as

$$\frac{C_e}{q_e} = \frac{1}{Q_0 K_L} + \frac{1}{Q_0} C_e \quad (4)$$

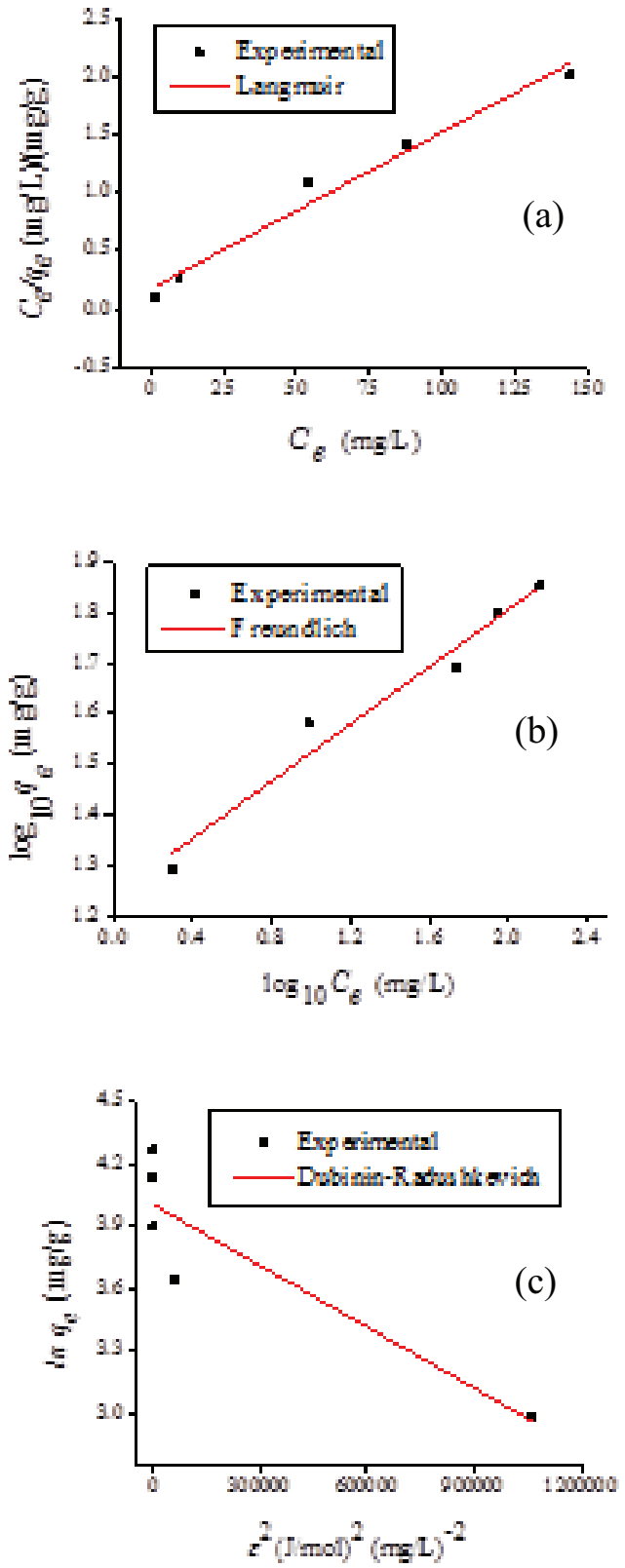

Fig. 8. Isotherm plot of PKB for the adsorption of Cr(VI) solution at equilibrium Cr(VI) concentrations. (a) Langmuir isotherm, (b) Freundlich isotherm and (c) Dubinin–Radushkevitch isotherm.

where 'q_e' represents the equilibrium adsorption capacity in mg/g, 'C_e' represents the equilibrium concentration of metal ion (mg/L), 'Q_0' is the monolayer adsorption capacity (mg/g) and 'K_L' denotes the Langmuir isotherm constant (L/mg). From the K_L values the separation factor 'R_L' can be determined as

$$R_L = \frac{1}{1 + K_L C_o} \tag{5}$$

The separation factor value is significant in determining the nature of the adsorption process. If R_L lies between 0 and 1, the adsorption may be favorable, it is unfavorable if it is 1 and the process is irreversible if the value is 0. Fig. 8(a) shows the linear isotherm plot of the ratio of equilibrium Cr(VI) concentration and equilibrium adsorption capacity of PKB versus equilibrium Cr(VI) concentration constructed using OriginPro 8.5 (OriginLab, USA). From Table 2, it is apparent that the regression value is 0.968 which is comparatively higher than the other isotherm models. The monolayer adsorption capacity of PKB was found to be 73.96 mg/g. Lower value of K_L, 0.0789 L/mg, showed that there was a higher affinity between chromium ions and the biosorbent. R_L value of 0.112–0.024 for initial metal concentrations of 100–500 mg/L Cr(VI) showed that the adsorption process was favorable.

3.6.2. Freundlich isotherm

Multilayer adsorption is explained by Freundlich isotherm which assumes that the surface of the adsorbing

Table 2
Isotherm parameters of PKB for adsorption of Cr(VI)

Isotherm analysis	Parameters	PK biomass
Langmuir	Q_o (mg/g)	73.96
	K_L (L/mg)	0.0789
	R_L (100–500 mg/L)	0.112–0.024
	Goodness of fit	
	R^2	0.96809
	Number of points	5
	Degrees of freedom	3
	Residual sum of squares	0.06145
Freundlich	K_F (mg/g)(L/mg)$^{1/n_F}$	17.33
	n_F	3.525
	Goodness of fit	
	R^2	0.95794
	Number of points	5
	Degrees of freedom	3
	Residual sum of squares	0.0062
Dubinin–Radushkevitch	Q_m (mg/g)	54.830
	K (mol^2/J^2)	9.834E–7
	E (kJ/mol)	0.713
	Goodness of fit	
	R^2	0.75624
	Number of points	5
	Degrees of freedom	3
	Residual sum of squares	0.19053

material is heterogeneous with varying affinity towards the adsorbing ligands [39]. The linear form of Freundlich isotherm model is expressed as

$$\log_{10} q_e = \log_{10} K_F + \frac{1}{n_F}\log_{10} C_e \quad (6)$$

where K_F and n_F represents the Freundlich isotherm constant $(mg/g)(L/mg)^{1/n}{}_F$ and Freundlich exponent (dimensionless), respectively. Freundlich constant (n_F) represents the degree to which adsorption deviates from linearity. From the linear isotherm plotted (Fig. 8(b)), the value of K_F was found to be 17.33. Lower value of $1/n_F$ depicted that the Cr(VI) over surface of PKB is favorable. Regression value of 0.957 (Table 2) represented a fit of Freundlich isotherm comparable with Langmuir isotherm depicted that the adsorption process may be multilayer as well.

3.6.3. Dubinin–Radushkevich (D–R) isotherm

The linear DR isotherm model equation is given by [40]

$$\ln q_e = \ln Q_m - K\varepsilon^2 \quad (7)$$

where Q_m symbolizes the maximum adsorption capacity (mg/g), K symbolizes the activity coefficient (mol^2/J^2), ε denotes the Polanyi potential which is obtained by the equation:

$$\varepsilon = RT(\ln(1 + C_e^{-1})) \quad (8)$$

where R represents the universal gas constant in J/mol K and T represents the absolute temperature (K). Q_m and K values estimated by plot (Fig. 8(c)) of $\log(q_e)$ versus ε^2 were found to be 54.830 mg/g and 9.834E–7 mol^2/J^2, respectively. An important parameter obtained from DR model is apparent adsorption energy, E (kJ/mol) which is calculated by the expression

$$E = \frac{1}{\sqrt{2K}} \quad (9)$$

If $1 < E < 16$ kJ/mol, the adsorption process occurs by physical adsorption and if $E > 16$ kJ/mol, the adsorption process occurs by chemisorption. If $8 < E < 16$ kJ/mol, the mechanism predominantly involves ion exchange [41]. The DR constants were determined and are depicted in Table 2. However, the value of E for PKB was 0.713 kJ/mol, which indicated that the biosorption process occurs by physisorption.

3.7. Kinetic studies

3.7.1. Pseudo-first order

The linear form of pseudo-first-order kinetic model is given by

$$\log(q_e - q_t) = \log q_e - \frac{k_1}{2.303}t \quad (10)$$

where k_1 is the pseudo-first-order rate constant (min^{-1}), q_e is the equilibrium adsorption capacity (mg/g) and q_t is the adsorption capacity (mg/g) [42]. Table 3 depicts various kinetic model parameters and regression values of the model. q_e values calculated from the plot of $\log(q_e–q_t)$ versus t did not correlated well with the experimental values. The R^2 values obtained for pseudo-first-order model were found to be less than the R^2 values for other kinetic models, which reveal that the adsorption of Cr(VI) upon PKB does not obey pseudo-first-order reaction.

3.7.2. Pseudo-second order

The pseudo-second-order kinetic model is represented by the equation:

$$\frac{t}{q_t} = \frac{1}{k_2 q_e^{\,2}} + \frac{t}{q_e} \quad (11)$$

where k_2 (g/mg/min) denotes the pseudo-second-order rate constant [43]. The linear form of the pseudo-second-order kinetic model is shown in Fig. 9(a) at different initial Cr(VI) concentrations. There was a good correlation in the experimental and calculated q_e values with the increase in the concentration of Cr(VI) (Table 3). The R^2 values obtained for pseudo-second-order model were comparatively higher than the other kinetic models analyzed. Hence, the adsorption process of Cr(VI) by PKB involved pseudo-second-order reaction with sharing of electrons between sorbent and sorbate.

3.7.3. Intraparticle diffusion kinetic model

Intraparticle diffusion model that represents the rate limiting steps is represented by the equation:

$$q_t = k_{id} t^{1/2} + C \quad (12)$$

Table 3
Kinetic parameters of PKB for Cr(VI) removal

C_o (mg/g)	Pseudo-first order			Pseudo-second order			Intraparticle diffusion	
	k_1 (min^{-1})	q_e (mg/g)	R^2	k_2 (g/mg/min)	q_e (mg/g)	R^2	k_{id} ($mg/g/min^{1/2}$)	R^2
100	0.013	1.476	0.662	0.216	19.60	0.999	1.07888	0.976
200	0.017	1.2918	0.882	0.039	35.71	0.999	4.05558	0.934
300	0.0207	1.5980	0.751	0.137	49.26	0.999	4.61159	0.965
400	0.0237	1.6865	0.762	2.77×10^{-5}	62.50	0.999	6.11128	0.977
500	0.0207	1.5427	0.780	2.84×10^{-5}	71.42	0.999	7.04445	0.973

where k_{id} is the intraparticle diffusion rate constant (mg/g/min$^{1/2}$), C is the intercept [44]. The q_e values calculated from the model plot were not close to experimental values. R^2 values are lower than pseudo-second-order and pseudo-first-order kinetic models (Table 3). Also, the plot between $t^{1/2}$ and q_t did not passed through the origin and multilinearity resulted which is clearly shown in Fig. 9(b). It was inferred that the process of Cr(VI) adsorption upon the PKB surface may not be solely controlled by intraparticle diffusion [44].

3.8. Thermodynamic studies

Influence of temperature for various Cr(VI) concentrations has been studied and shown in Fig. 10(a). It was determined that the adsorption capacity gradually increased with the simultaneous increase in the temperature and initial Cr(VI) concentration. The rise in biosorption capacity may be due to the increased mobility of the ions and modification that would have taken place in the functional groups of the biosorbent which makes them more available for contacting ions with the increase in temperature [45].

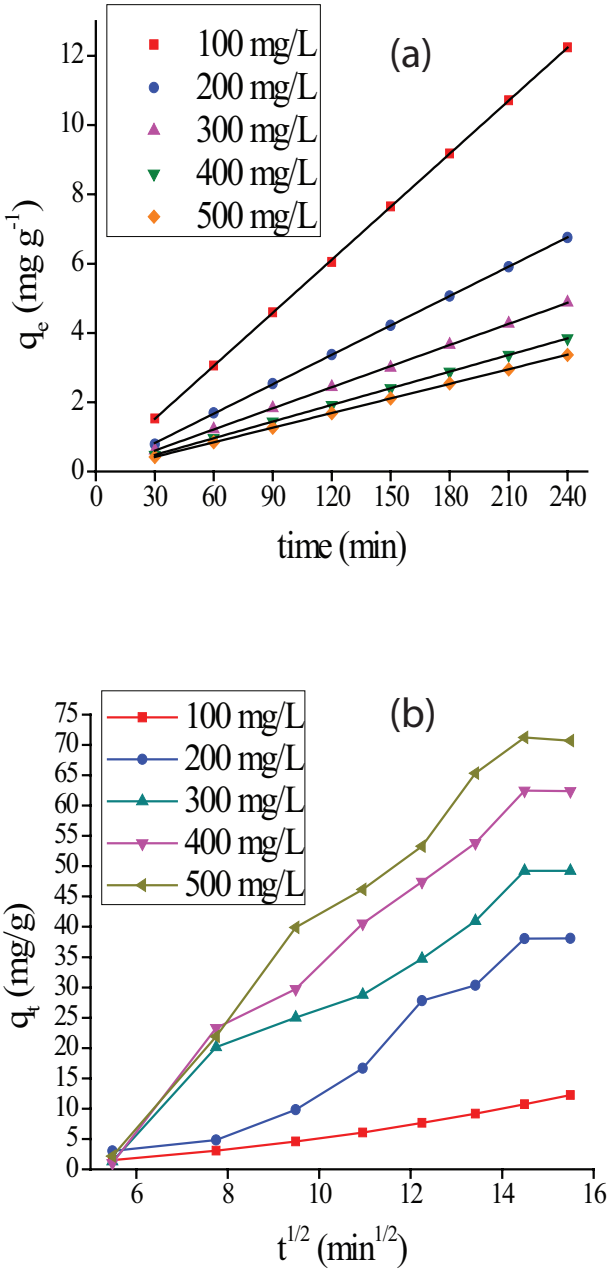

Fig. 9. (a) Pseudo-second-order plot and (b) intraparticle diffusion plot.

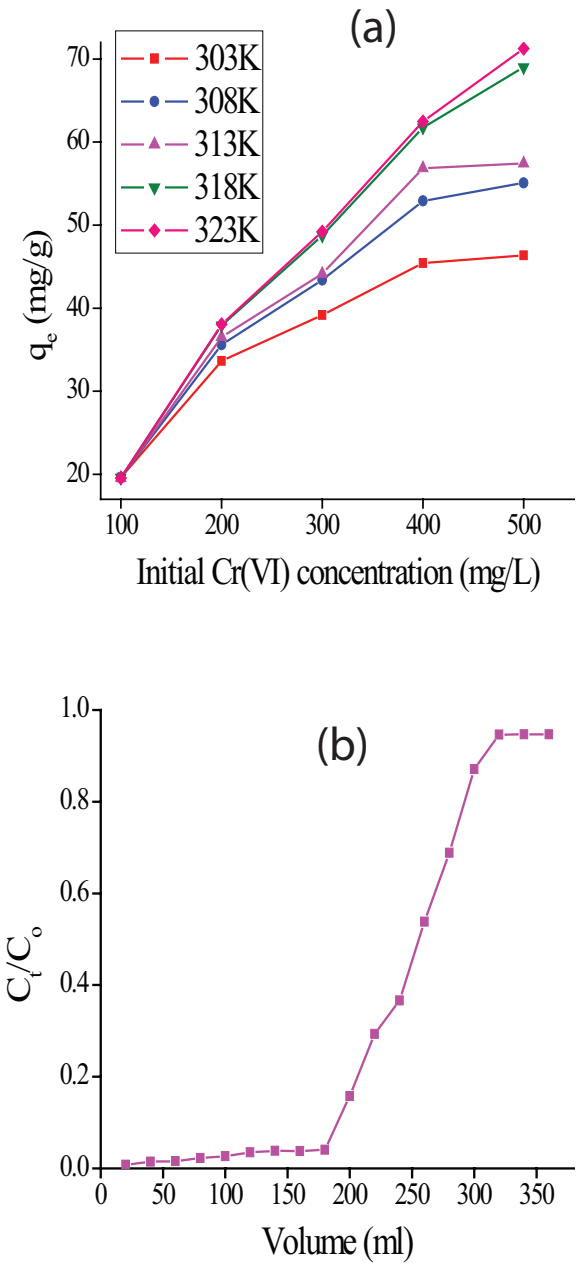

Fig. 10. (a) Influence of temperature at various concentrations of Cr(VI) and (b) break through curve of PKB in column studies.

Gibbs free energy (Δ*G*°), enthalpy (Δ*H*°) and entropy (Δ*S*°) were calculated using the following equations [46]:

$$\Delta G^{o} = -RT\ln K_C \tag{13}$$

where '*T*' denotes absolute temperature (K) and '*R*' represents universal gas constant (8.314 J/mol/K) and K_C symbolizes the distribution coefficient given by

$$\ln K_C = -\frac{\Delta H^{o}}{RT} + \frac{\Delta S^{o}}{R} \tag{14}$$

$$K_C = \frac{q_e}{C_e} \tag{15}$$

Table 4 shows the thermodynamic parameters estimated from the temperature studies at various metal concentrations. The negative Δ*G*° values indicated the spontaneous nature of the biosorption process [47]. The Δ*H*° values were negative which indicated exothermic nature of process. Further, the Δ*S*° values were negative which revealed the stable bonding of Cr(VI) on PKB surface [48]. This may be due to the decrease in the randomness and movement of molecules at the sorbent–sorbate interface.

3.9. Desorption and regeneration studies

Desorption experiments were carried out after adsorption studies for a period of 6 h using 0.1 N NaOH as desorption agent at 100 rpm, 303 K. Maximum desorption was achieved in 300 min and no further increase in desorption was found. The regenerated sorbent was filtered and adsorption experiments were performed with optimized conditions of 100 mg/L initial metal concentration, 2.0 pH, 303 K and 100 rpm. These steps were repeated until considerable adsorption of Cr(VI) was attained. The maximum desorption percentage in the first run was 47.61 and it was reduced to 32.46 in the second run (Table 5). The regenerated PKB at the first run showed a maximum of 82.30% Cr(VI) removal and in the second run of regeneration, it showed only 31.80% Cr(VI) removal. The decrease in the desorption percentage might be due to the change of functional groups or Cr binding groups after continuous exposure of desorbing agent and Cr(VI) solution. Tremendous decrease in the removal percentage post-desorption was due to the unavailability of binding sites for chromium ions.

3.10. Continuous column studies

Continuous column studies of Cr(VI) removal was performed using a packed bed column of PKB at 5 cm height.

Table 4
Thermodynamic parameters of PKB for Cr(VI) removal

Temperature (K)	Δ*G*° (kJ/mol)					Δ*H*° (kJ/mol)	Δ*S*° (kJ/mol K)
	Initial metal concentration (mg/L)						
	100	200	300	400	500		
303	−24.98	−8.73	−1.83	−1.30	−0.81	−59.07	−0.106
308	−29.33	−8.75	−1.97	−1.48	−0.90	−101.28	−0.303
313	−24.66	−5.51	−1.44	−1.27	−0.70	−11.22	−0.030
318	−25.05	−4.57	−1.55	−1.20	−0.81	−5.7	−0.014
323	−24.36	−3.21	−1.27	−1.08	−0.71	−2.6	−0.006

Table 5
Desorption and regeneration data of PKB using 100 ppm initial Cr(VI) concentration

Time (min)	Cycle 1		Cycle 2	
	Chromium desorption (%)	Chromium adsorption (%)	Chromium desorption (%)	Chromium adsorption (%)
30	11.85	1.79	15.91	0.35
60	12.39	15.63	14.16	2.15
90	21.31	20.12	11.02	6.64
120	42.04	39.89	14.58	12.93
150	45.29	50.67	15.77	14.73
180	42.42	70.88	26.04	24.61
210	45.45	81.22	36.12	28.12
240	45.45	82.12	33.41	30.90
300	47.61	82.30	32.69	31.80
360	47.61	82.30	32.69	30.90

Fig. 10(b) shows breakthrough curve of the PKB obtained after the passage of 100 mg/L of Cr(VI) solution through the column. Breakpoint curve was constructed from a plot between volumes of outlet collected versus C_t/C_o. It was found that a packed bed made of 4.5 g of PKB was capable of remediating 180 mL of Cr(VI) solution under given conditions. Hence, PKB can be used as an ecofriendly sorbent for treating real Cr(VI) containing aqueous effluents.

3.11. Economics of using PKB

The cost of the Cr(VI) biosorption from wastewater is primarily based on factors such as convenient availability of biosorbent, amount of biosorbent available, its biosorption capacity and competency. The expense of activated carbons conventionally deployed for wastewater remediation is approximately $1,400–1,800/tons in India. The PKB, a waste biomass, was obtained from the Nehru Park, Shillong, Meghalaya, India, for negligible cost. The cumulative cost of preparing the biosorbent material including water and electrical energy would be $75/tons. In conclusion, the prepared biosorbent PKB offers an affordable yet efficient alternative strategy for the disposal of Cr(VI) from wastewater.

4. Conclusion

Removal of Cr(VI) from simulated solutions has been investigated using a novel biosorbent PKB. The physicochemical characteristic studies of the biosorbent showed that it has a considerable surface area and pore volume with several functional groups embedded over their surface which are prone to metal binding. The biosorption of Cr(VI) onto PKB has been confirmed by FTIR, FESEM–EDX, XRD and ESR studies. It was depicted that the Cr(VI) removal was highest at an optimum initial solution pH 2.0, temperature 303 K, PKB particle size of <300 μm, PKB dose of 0.5 g/L, contact time 210 min, initial chromium concentration of 500 mg/L at a constant agitation speed of 100 rpm. Isotherm studies obeyed Freundlich model which imply that the biosorption is predominantly multilayer over a heterogeneous sorbent surface. Maximum adsorption capacity of the biosorbent was 73.96 mg/g which is comparatively higher than reported in the literature (Table 6). Kinetic parameters fitted well with pseudo-second-order kinetics. Thermodynamic parameters revealed that the biosorption process is spontaneous, stable and exothermic. Desorption studies with NaOH revealed that the biosorbent is reusable. Continuous packed bed column studies showed that the *P. kesiya* cone biosorbent is an environment-friendly option to abate Cr(VI) from synthetic Cr(VI) solutions.

Table 6
Comparison of adsorption capacities of various biosorbent with PKB

Biosorbents	pH	q_e (mg/g)	References
Rice straw	2.0	3.15	[49]
Pine needles	2.0	21.50	[50]
Modified litchi peels	1.0	9.55	[51]
Pineapple leaves	2.0	18.77	[52]
Artemisia absinthium (herb)	2.0	46.99	[53]
Cone biomass of *Thuja orientalis*	1.5	49.0	[54]
Potato peel	2.5	3.28	[55]
Pinus kesiya cone biomass (PKB)	2.0	73.96	This study

Symbols

q_t	—	Biosorption capacity, mg/g
q_e	—	Biosorption capacity at equilibrium, mg/g
C_o	—	Initial metal concentration, mg/L
C_e	—	Metal concentration at equilibrium, mg/L
C_t	—	Metal concentration at *t* time, mg/L
V	—	Volume of the metal solution, L
m	—	Weight of the biosorbent, g
Q_o	—	Biosorption capacity from Langmuir model, mg/g
K_L	—	Langmuir isotherm constant, L/mg
R_L	—	Separation factor, dimensionless
K_F	—	Freundlich isotherm constant, (mg/g)(L/mg)$^{1/n}$
n_F	—	Freundlich exponent, dimensionless
Q_m	—	Maximum biosorption capacity from Dubinin–Radushkevich model, mg/g
K	—	Constant related to the mean free energy of biosorption, mol^2/kJ^2
ε	—	Polanyi potential of Dubinin–Radushkevich model, kJ/mol
R	—	Universal gas constant, 8.314 J/mol/K
T	—	Temperature, K
E	—	Apparent adsorption energy, kJ/mol
k_1	—	Pseudo-first-order constant, min^{-1}
k_2	—	Pseudo-second-order constant, g/mg/min
k_{id}	—	Intraparticle diffusion rate constant, mg/g/min$^{1/2}$
C	—	Intercept of intraparticle diffusion model
$\Delta G°$	—	Free energy change, kJ/mol
$\Delta H°$	—	Enthalpy change, kJ/mol
$\Delta S°$	—	Entropy change, kJ/mol
K_C	—	Distribution coefficient

Acknowledgments

The support of The Central Instrumentation Facility, Indian Institute of Technology Guwahati is gratefully acknowledged. The financial support of Department of Science and Technology, Ministry of Science and Technology, India (Grant no. SERC/ET-0356/2012) is gratefully acknowledged.

References

[1] A.A. Alqadami, M. Naushad, Z.A. Alothman, A.A. Ghfar, Novel metal-organic framework (MOF) based composite material for the sequestration of U(VI) and Th(IV) metal ions from aqueous environment, ACS Appl. Mater. Interfaces, 9 (2017) 36026–36037.
[2] M. Naushad, T. Ahamad, B.M. Al-Maswari, A. Abdullah, A. Saad, M. Alshehri, Nickel ferrite bearing nitrogen-doped mesoporous carbon as efficient adsorbent for the removal of highly toxic metal ion from aqueous medium, Chem. Eng. J., 330 (2017) 1351–1360.

[3] World Health Organization Division of Operational Support in Environmental, Guidelines for Drinking-Water Quality. Vol. 2, Health Criteria and Other Supporting Information : Addendum, 1998. Available at: http://www.who.int/iris/handle/10665/63844.
[4] A.K. Shanker, B. Venkateswarlu, Chromium: Environmental Pollution, Health Effects and Mode of Action, Encyclopedia of Environmental Health, Elsevier, J.O. Nriagu, 2011, pp. 650–659.
[5] J.W. Moore, C.L. Stanitski, Chemistry: The Molecular Science, Cengage Learning, 2014, 1272 pages.
[6] D.E. Kimbrough, Y. Cohen, A.M. Winer, L. Creelman, C. Mabuni, A critical assessment of chromium in the environment, Crit. Rev. Environ. Sci. Technol., 29 (1999) 1–46.
[7] G. Agarwal, H. Bhuptawat, S. Chaudhari, Biosorption of aqueous chromium(VI) by *Tamarindus indica* seeds, Bioresour. Technol., 97 (2006) 949–956.
[8] D. Mohan, C.U. Pittman, Activated carbons and low cost adsorbents for remediation of tri- and hexavalent chromium from water, J. Hazard. Mater., 137 (2006) 762–811.
[9] L. Sellaoui, F.E. Soetaredjo, S. Ismadji, E.C. Lima, G.L. Dotto, A.B. Lamine, A. Erto, New insights into single-compound and binary adsorption of copper and lead ions on a treated sea mango shell: experimental and theoretical studies, PCCP, 19 (2017) 25927–25937.
[10] A. Kumar, A. Kumar, G. Sharma, A.H. Al-Muhtaseb, M. Naushad, A.A. Ghfar, F.J. Stadler, Quaternary magnetic BiOCl/g-C_3N_4/Cu_2O/Fe_3O_4 nano-junction for visible light and solar powered degradation of sulfamethoxazole from aqueous environment, Chem. Eng. J., 334 (2018) 462–478.
[11] A. Kumar, C. Guod, G. Sharma, D. Pathania, M. Naushad, S. Kalia, P. Dhiman, Magnetically recoverable ZrO_2/Fe_3O_4/chitosan nanomaterials for enhanced sunlight driven photoreduction of carcinogenic Cr (VI) and dechlorination & mineralization of 4-chlorophenol from simulated waste water, RSC Adv., 6 (2016) 13251–13263.
[12] A. Dąbrowski, Adsorption—from theory to practice, Adv. Colloid Interface Sci., 93 (2001) 135–224.
[13] R. Han, J. Zhang, W. Zou, J. Shi, H. Liu, Equilibrium biosorption isotherm for lead ion on chaff, J. Hazard. Mater., 125 (2005) 266–271.
[14] L. Sellaoui, D.S.P. Franco, G.L. Dotto, É.C. Lima, A.B. Lamine, Single and binary adsorption of cobalt and methylene blue on modified chitin: application of the Hill and exclusive extended Hill models, J. Mol. Liq., 233 (2017) 543–550.
[15] Y. Li, B. Zhao, L. Zhang, R. Han, Biosorption of copper ion by natural and modified wheat straw in fixed-bed column, Desal. Wat. Treat., 51 (2013) 5735–5745.
[16] N. Sivarajasekar, K. Balasubramani, N. Mohanraj, J.P. Maran, S. Sivamani, P.A. Koya, V. Karthik, Fixed-bed adsorption of atrazine onto microwave irradiated *Aegle marmelos* Correa fruit shell: statistical optimization, process design and breakthrough modelling, J. Mol. Liq., 241 (2017) 823–830.
[17] B. Preetha, T. Viruthagiri, Batch and continuous biosorption of chromium(VI) by *Rhizopus arrhizus*, Sep. Purif. Technol., 57 (2007) 126–133.
[18] V.K. Gupta, A. Rastogi, Biosorption of hexavalent chromium by raw and acid-treated green alga *Oedogonium hatei* from aqueous solutions, J. Hazard. Mater., 163 (2009) 396–402.
[19] K. Kayalvizhi, K. Vijayaraghavan, M. Velan, Biosorption of Cr(VI) using a novel microalga *Rhizoclonium hookeri*: equilibrium, kinetics and thermodynamic studies, Desal. Wat. Treat., 56 (2015) 194–203.
[20] R. Senthilkumar, K. Vijayaraghavan, J. Jegan, M. Velan, Batch and column removal of total chromium from aqueous solution using *Sargassum polycystum*, Environ. Prog. Sustainable Energy, 29 (2010) 334–341.
[21] X. Wang, Z. Li, S. Tao, Removal of chromium (VI) from aqueous solution using walnut hull, J. Environ. Manage., 90 (2009) 721–729.
[22] V.K. Gupta, D. Pathania, S. Agarwal, S. Sharma, Removal of Cr(VI) onto *Ficus carica* biosorbent from water, Environ. Sci. Pollut. Res., 20 (2013) 2632–2644.
[23] G. Sharma, M. Naushad, A.H. Al-Muhtaseb, A. Kumar, M.R. Khan, S. Kalia, S.M. Bala, A. Sharma, Fabrication and characterization of chitosan-crosslinked-poly(alginic acid) nanohydrogel for adsorptive removal of Cr(VI) metal ion from aqueous medium, Int. J. Biol. Macromol., 95 (2017) 484–493.
[24] S.M. Ickert-Bond, Cuticle Micromorphology of *Pinus krempfii* Lecomte (Pinaceae) and additional species from Southeast Asia, Int. J. Plant Sci., 161 (2000) 301–317.
[25] H. Choudhury, Development of an Embryogenic System for Mass Propagation of *Pinus kesiya* Royle ex Gord and Field Performance of the Regenerants, Ph.D. Thesis, North-Eastern Hill University, Shillong, Meghalaya, 2002.
[26] K. Li, S. Tian, J. Jiang, J. Wang, X. Chen, F. Yan, Pine cone shell-based activated carbon used for CO_2 adsorption, J. Mater. Chem. A, 4 (2016) 5223–5234.
[27] S. Rangabhashiyam, N. Selvaraju, Evaluation of the biosorption potential of a novel *Caryota urens* inflorescence waste biomass for the removal of hexavalent chromium from aqueous solutions, J. Taiwan Inst. Chem. Eng., 47 (2015) 59–70.
[28] N. Saranya, E. Nakeeran, M.S.G. Nandagopal, N. Selvaraju, Optimization of adsorption process parameters by response surface methodology for hexavalent chromium removal from aqueous solutions using *Annona reticulata* Linn peel microparticles, Water Sci. Technol., 75 (2017) 2094–2107.
[29] E. Nakkeeran, N. Saranya, M.S.G. Nandagopal, A. Santhiagu, N. Selvaraju, Hexavalent chromium removal from aqueous solutions by a novel powder prepared from *Colocasia esculenta* leaves, Int. J. Phytorem., 18 (2016) 812–821.
[30] G. Gebrehawaria, A. Hussen, V.M. Rao, Removal of hexavalent chromium from aqueous solutions using barks of *Acacia albida* and leaves of *Euclea schimperi,* Int. J. Environ. Sci. Technol., 12 (2015) 1569–1580.
[31] R. Jin, Y. Liu, G. Liu, T. Tian, S. Qiao, J. Zhou, Characterization of product and potential mechanism of Cr(VI) reduction by anaerobic activated sludge in a sequencing batch reactor, Sci. Rep., 7 (2017) 1681.
[32] S. Kuppusamy, P. Thavamani, M. Megharaj, K. Venkateswarlu, Y.B. Lee, R. Naidu, Potential of *Melaleuca diosmifolia* leaf as a low-cost adsorbent for hexavalent chromium removal from contaminated water bodies, Process Saf. Environ. Prot., 100 (2016) 173–182.
[33] V. Nair, A. Panigrahy, R. Vinu, Development of novel chitosan–lignin composites for adsorption of dyes and metal ions from wastewater, Chem. Eng. J., 254 (2014) 491–502.
[34] R. Saha, B. Saha, Removal of hexavalent chromium from contaminated water by adsorption using mango leaves (*Mangifera indica*), Desal. Wat. Treat., 52 (2014) 1928–1936.
[35] G. Moussavi, B. Barikbin, Biosorption of chromium(VI) from industrial wastewater onto pistachio hull waste biomass, Chem. Eng. J., 162 (2010) 893–900.
[36] I. Ullah, R. Nadeem, M. Iqbal, Q. Manzoor, Biosorption of chromium onto native and immobilized sugarcane bagasse waste biomass, Ecol. Eng., 60 (2013) 99–107.
[37] I. Langmuir, The adsorption of gases on plane surfaces of glass, mica and platinum, J. Am. Chem. Soc., 40 (1918) 1361–1403.
[38] N. Sivarajasekar, R. Baskar, T. Ragu, K. Sarika, N. Preethi, T. Radhika, Biosorption studies on waste cotton seed for cationic dyes sequestration: equilibrium and thermodynamics, Appl. Water Sci., 7 (2017) 1987–1995.
[39] H. Freundlich, Über die Adsorption in Lösungen, Z. Phys. Chem., 57U (1907) 385–470.
[40] K. Sing, Reporting physisorption data for gas/solid systems with special reference to the determination of surface area and porosity (Recommendations 1984), Pure Appl. Chem., 57 (1985) 603–619.
[41] S. Aytas, D.A. Turkozu, C. Gok, Biosorption of uranium(VI) by bi-functionalized low cost biocomposite adsorbent, Desalination, 280 (2011) 354–362.
[42] S. Lagergren, Zurtheorie der sogenannten adsorption gelosterstoffe, Kongl. Sv.Vet. Akad. Handlingar, 24 (1898) 1–39.
[43] Y.S. Ho, G. McKay, Pseudo-second order model for sorption processes, Process Biochem., 34 (1999) 451–465.

[44] W. Weber, J. Morris, Advances in Water Pollution Research: Removal of Biologically Resistant Pollutants from Waste Waters by Adsorption, Proceedings of the International Conference On Water Pollution Symposium, vol. 2, 1962, pp. 231–266.
[45] S. Rangabhashiyam, N. Selvaraju, Adsorptive remediation of hexavalent chromium from synthetic wastewater by a natural and $ZnCl_2$ activated *Sterculia guttata* shell, J. Mol. Liq., 207 (2015) 39–49.
[46] A.S. Özcan, S. Tunali, T. Akar, A. Özcan, Biosorption of lead(II) ions onto waste biomass of *Phaseolus vulgaris* L., estimation of the equilibrium, kinetic and thermodynamic parameters, Desalination, 244 (2009) 188–198.
[47] H.N. Tran, S.-J. You, H.-P. Chao, Thermodynamic parameters of cadmium adsorption onto orange peel calculated from various methods: a comparison study, J. Environ. Chem. Eng., 4 (2016) 2671–2682.
[48] A. Kumar, H.M. Jena, Adsorption of Cr(VI) from aqueous solution by prepared high surface area activated carbon from Fox nutshell by chemical activation with H_3PO_4, J. Environ. Chem. Eng., 5 (2017) 2032–2041.
[49] H. Gao, Y. Liu, G. Zeng, W. Xu, T. Li, W. Xia, Characterization of Cr(VI) removal from aqueous solutions by a surplus agricultural waste—rice straw, J. Hazard. Mater., 150 (2008) 446–452.
[50] M. Dakiky, M. Khamis, A. Manassra, M. Mer'eb, Selective adsorption of chromium(VI) in industrial wastewater using low-cost abundantly available adsorbents, Adv. Environ. Res., 6 (2002) 533–540.
[51] Y. Yi, J. Lv, Y. Liu, G. Wu, Synthesis and application of modified Litchi peel for removal of hexavalent chromium from aqueous solutions, J. Mol. Liq., 225 (2017) 28–33.
[52] J. Ponou, J. Kim, L.P. Wang, G. Dodbiba, T. Fujita, Sorption of Cr(VI) anions in aqueous solution using carbonized or dried pineapple leaves, Chem. Eng. J., 172 (2011) 906–913.
[53] R.A.K. Rao, S. Ikram, M.K. Uddin, Removal of Cr(VI) from aqueous solution on seeds of *Artimisia absinthium* (novel plant material), Desal. Wat. Treat., 54 (2015) 3358–3371.
[54] E. Oguz, Adsorption characteristics and the kinetics of the Cr(VI) on the *Thuja orientalis*, Colloids Surf., A, 252 (2005) 121–128.
[55] F. Mutongo, O. Kuipa, P.K. Kuipa, Removal of Cr(VI) from aqueous solutions using powder of potato peelings as a low cost sorbent, Bioinorg. Chem. Appl., 2014 (2014) 1–7.